HHS Public Access

Author manuscript

AJNR Am J Neuroradiol. Author manuscript; available in PMC 2020 November 01.

Published in final edited form as:

AJNR Am J Neuroradiol. 2019 November ; 40(11): 1796–1803. doi:10.3174/ajnr.A6253.

MRI Features of Histologically Diagnosed Supratentorial PNET And Pineoblastomas In Correlation with Molecular Diagnoses and Outcomes: A Report from the Children's Oncology Group ACNS0332 Trial.

Alok Jaju, MD,
Attending Radiologist, Ann and Robert H Lurie Children's Hospital of Chicago, Assistant Professor, Northwestern University Feinberg School of Medicine.

Eugene I. Hwang, MD,
Children's National Health System, Washington, DC, USA.

Marcel Kool,
German Cancer Research Center, Heidelberg, Baden-Württemberg, DE.

David Capper,
University Hospital Heidelberg, Heidelberg, Baden-Württemberg, DE.

Lukas Chavez,
University of California San Diego, La Jolla, CA, USA.

Sebastian Brabetz,
German Cancer Research Centre, Heidelberg, Baden-Württemberg, DE

Catherine Billups, MS,
St Jude Children's Research Hospital, Memphis, TN, USA

Yimei Li, PhD,
St Jude Children's Research Hospital, Memphis, TN, USA

Maryam Fouladi, MD,
Cincinnati Children's Hospital, Cincinnati, OH, USA

Roger J. Packer, MD,
Children's National Health System, Washington, DC, USA.

Stefan M. Pfister,
German Cancer Research Center, Heidelberg, Baden-Württemberg, DE.

James M. Olson, MD,
Fred Hutchinson Cancer Research Center, Seattle, WA, USA

(Corresponding author) Attending Radiologist, Ann and Robert H Lurie Children's Hospital of Chicago, Assistant Professor, Northwestern University Feinberg School of Medicine., Address: 225 E. Chicago Ave, Box #9, Chicago, IL 60611., Phone: 312-227-3501 (Office); 314-488-1759 (Cell), Fax: 312-227-9784.

Meeting presentation:
Some data from this study will be included in an oral presentation accepted for the ASNR Annual Meeting in May 2019.

Linda A. Heier, MD
New York Presbyterian Hospital, New York, NY, USA 10021

Abstract

Background and Purpose: Supratentorial primitive neuroectodermal tumors (PNET) and pineoblastomas (PBL) have traditionally been grouped together for treatment purposes. Molecular profiling of these tumors has revealed a number of distinct entities and led to the term 'CNS-PNET' being removed from the 2016 WHO classification. The purpose of this study is to describe the MRI findings of histologically-diagnosed PNETs and PBLs and correlate them with molecular diagnoses and outcomes.

Methods: Histologically-diagnosed PNET and PBL were enrolled on this Children's Oncology Group phase 3 trial, and molecular classification retrospectively completed using DNA methylation profiling. MRI features were systematically studied and correlated with molecular diagnoses and survival.

Results: Out of the 85 patients enrolled, 56 met the inclusion criteria, of which 28 tumors were in pineal and 28 in non-pineal locations. Methylation profiling revealed a variety of diagnoses including pineoblastomas (n=27), high grade gliomas (n=17), embryonal tumors (n=7), atypical teratoid rhabdoid tumors (n=3) and ependymomas (n=2). Based on this, 39% overall and 71% of non-pineal tumor diagnoses were discrepant with histopathology. Tumor location, size, margins and edema were predictors of embryonal versus non-embryonal tumors. Larger size and ill-defined margins correlated with poor event-free survival, while metastatic disease by MRI did not.

Conclusion: In non-pineal locations, only a minority of histologically diagnosed PNET are embryonal tumors, and therefore high grade glioma or ependymoma should be high on the radiographic differential. An understanding of molecularly defined tumor entities, their relative frequencies and locations will help the radiologist make more accurate predictions of the tumor types.

Introduction:

Historically, supratentorial primitive neuroectodermal tumors of the central nervous system (CNS-PNET) and pineoblastomas (PBL) have been considered to be embryonal tumors histopathologically similar to medulloblastomas, although the classification has been a topic of much debate.[1,2] CNS-PNET and PBL have thus been treated as a single group using protocols designed for high-risk medulloblastomas.[3,4] In recent years, molecular profiling using genome-wide DNA methylation of histopathologically diagnosed CNS-PNETs have revealed a wide spectrum of distinct molecular entities, including high-grade gliomas (HGG), atypical teratoid rhabdoid tumors (ATRT), ependymomas (EP), and at least four new molecular entities.[5–7] The 2016 World Health Organization (WHO) classification has removed CNS-PNET as a diagnostic category, in part substituting it with a broad group termed 'CNS embryonal tumors, NOS', in addition to more specific entities, such as embryonal tumor with multi-layered rosettes (ETMR).[8]

Molecularly defined entities may more accurately predict clinical outcomes when compared with standard histopathological diagnosis in CNS-PNET, [7] as well as in other pediatric CNS

tumors such as medulloblastoma and ependymoma.[9,10] However, practical barriers such as cost, availability, timeliness of results, and assay certification can hamper utilization. In recent years, there has been growing interest in correlating imaging features with molecular markers in an attempt to identify imaging phenotypes that may serve as surrogates for molecular subtypes.[11,12] This radiogenomic approach has been applied with some success in CNS tumors such as glioblastomas [13,14], medulloblastomas,[15] ATRT,[16] as well as non-CNS tumors.[17]

The Children's Oncology Group (COG) study ACNS0332, a multi-center phase 3 prospective trial, investigated two approaches for treatment intensification - the addition of carboplatin during irradiation and the addition of adjuvant isotretinoin - in patients diagnosed with either CNS-PNET/PBL or high-risk medulloblastoma in two parallel randomized strata. The results from the completed CNS-PNET/PBL portion of the trial, including an analysis of molecular profiles and patient outcomes, have been published.[7] These results have shown that the molecularly diagnosed HGG had significantly worse survival compared to supratentorial embryonal tumors and PBL.[7] Thus, the distinction between these two categories is critical to the management of these patients.

As a part of this trial, magnetic resonance imaging (MRI) of the brain and spine were obtained at multiple time-points and submitted for central review. The current report focuses on the MRI features of CNS-PNET/PBL and their correlation with molecular subtypes and outcomes. Identifying reliable correlations would facilitate imaging-guided clinical decision making when molecular profiling is unavailable or delayed.

Methods:

Patient Cohort:

For the strata included in this report, children from 3 to 22 years were eligible who had newly diagnosed primary CNS-PNET or PBL by institutional pathologists per the 2007 World Health Organization (WHO) classification system, defined as undifferentiated or poorly differentiated tumors with the capacity for divergent differentiation. Subjects had minimum functional scores (Lansky/Karnofsky) of 30, adequate renal, marrow and hepatic function, and were staged with spinal CSF cytology and MRI of the brain and spine. Institutional review board approval and individual informed consent were obtained prior to enrollment, and the study was registered with ClinicalTrials.gov (NCT00392327).

Molecular analysis:

DNA methylation profiling was performed for all cases with sufficient tumor DNA using the Infinium HumanMethylation450 (450k) or the EPIC BeadChip arrays, and the tumors were classified using the recently developed brain diagnostic classifier algorithm (www.molecularneuropathology.org).[18] The methods are described in more detail in earlier publications.[5,7,19]

Neuroimaging guidelines and central review:

MRIs of the brain without and with contrast were obtained at diagnosis and after definitive surgery (within 72 hours). For patients who underwent stereotactic biopsy only, a postoperative MRI was not required. MRI of the spine with contrast was obtained within 10 days of surgery if done preoperatively, and within 28 days of surgery if done post-operatively. Additional MRIs of the brain and spine were obtained at the end of radiation therapy, end of maintenance chemotherapy, at relapse (if any), and at best response.

For this multi-institutional study, guidelines were provided for the technical parameters of MRI. The minimum recommended sequences for brain included sagittal and axial T1 weighted, axial T2 weighted, axial T2 FLAIR, axial diffusion weighted; and post contrast axial and sagittal T1 weighted. The minimum recommended sequences for spine included post contrast sagittal and axial T1 weighted. The studies were performed on a variety of scanners from different vendors, including both 1.5 and 3 Tesla field strengths, and varying technical parameters.

The MRI studies were retrospectively reviewed after treatment completion, by two experienced pediatric neuroradiologists by consensus (LH and AJ), blinded to the histopathological and molecular diagnosis. Only the MRI studies deemed technically acceptable by the central reviewers were included in this analysis, and there was no opportunity to obtain repeat or additional imaging because of the retrospective nature of the review. MRI features of the lesions were recorded including location, laterality, size, margins, surrounding edema, enhancement, cyst/necrosis, hemorrhage/calcification, and metastasis. The size was measured as the longest linear dimension in centimeters (cm). The margins were described as well-defined or ill-defined (>50% margins indistinct). The surrounding edema was assessed as absent, <2 cm from the tumor margin or >2 cm from the tumor margin. The extent of enhancement of the solid portion of the tumor was categorized subjectively as none, <25%, 25–75% and >75%. The degree of enhancement was subjectively assessed as none, mild, moderate or marked. The presence of cyst(s) or necrosis and low signal on T2 or GRE sequences suspicious for calcification or hemorrhage were noted and both these findings subjectively quantified as involving <25%, 25–50% or >50 % of the tumor.

The radiographic presence of intracranial and spinal metastasis was assessed, and in conjunction with CSF cytology, used to assign the M stage (modified Chang staging). Also, the post-operative MRIs were reviewed, and extent of resection classified as biopsy (<10%), partial (10–49%), subtotal (50–95%), radical subtotal (>95%), and gross total (no visible tumor on imaging).

Outcome analysis:

Event-free survival (EFS) was defined as the time interval from date of study enrollment to date of first event (disease progression or recurrence, second malignant neoplasm or death from any cause) or to the date of last follow-up for patients without events.

Statistical analysis:

The exact Wilcoxon rank sum test was used to compare continuous variables among patient groups. Fisher's exact test and the exact chi-square test were used to compare distributions of categorical variables. Outcome estimates were obtained using the method of Kaplan and Meier. The log rank test was used to compare outcome distributions. Cox regression was used to examine tumor size as a continuous predictor of outcome. Two-sided p-values are reported. Please note that patient numbers were quite small in some patient groups. Data frozen as of 12/31/2016 were used for this analysis.

Results:

Between March 2007 and August 2014, 85 patients with institutionally-diagnosed CNS-PNET/PBL were enrolled and randomized between the four trial regimens. Out of these, 56 patients met the inclusion criteria for the current analysis including availability of molecular classification by DNA methylation and complete imaging datasets.

Methylation profiling revealed a spectrum of molecular diagnoses broader than those found by histopathology (Table 1), and included PBL (n=27); HGG (n=17; including eight GBM_G34, five GBM_MYCN, two DMG_K27, two GBM_MID); ATRT (n=3; including two ATRT_SHH, one ATRT_MYC); CNS neuroblastoma with FOXR2 activation (n=3); ependymoma with positive RELA fusion (EPN-RELA, n=2); medulloblastoma with wnt activation (MB_WNT, n=1); ETMR (n=1); and high-grade neuroepithelial tumor with MN1 alteration (HGNET-MN1, n=1). One tumor could not be classified and was designated as embryonal tumor, NOS (ET NOS, n=1). The molecularly-diagnosed supratentorial embryonal tumors (ET) were grouped together with PBL and the combined group referred to as PBL/ET hereafter (n=37, including: 27 PBL, three CNS neuroblastoma, three ATRT, one MB, one ETMR, one HGNET and one ET NOS) (Table 1). The rest of the subgroups, including HGG and EPN, neither of which were intended for inclusion on the trial, were combined into one group, hereafter referred to as non-embryonal tumors (non-ET; n=19, including: 17 HGG and two EPN). Of note, ATRT although an 'embryonal tumor' has historically been considered a unique subset with specific treatment algorithms, and was also not intended for trial inclusion. However, keeping with the embryonal tumor definition, these are included under PBL/ET.

For the included 56 patients, the median age at diagnosis was nine years (range, 3–18 years). The median age for patients with molecularly-diagnosed PBL/ET was 8.6 years (range, 3–18 years), and that for patients with non-ET was 11.0 years (range 3.8–16.1 years), with no significant difference (p=0.21). There were 22 males (39%) and 34 females (61%) overall. In the PBL/ET group, there were 11 males (30%) and 26 females (70%), while in the non-ET group, there were 11 males (58%) and eight females (42%). The median age at diagnosis for pineoblastomas in our study was 8.7 years (range, 3–18 years).

Overall, 28 tumors involved the pineal region and 28 were extra-pineal (Table 2 and Fig 1). Amongst the extra-pineal tumors, 64% (18/28) belonged to the non-ET group, compared to only 7% (2/28) of the pineal region tumors (p<0.001). Twenty-four of the extra-pineal tumors were centered in the parenchyma and four within the ventricles. For the parenchymal

tumors, frontal lobe involvement was most common (56%), followed by parietal lobe (36%), with temporal and occipital lobe involvement being rare (7% each) (Fig 1).

Looking at the locations of individual tumor categories, almost all (26 out of 27) pineoblastomas were centered in the pineal cistern, with variable involvement of the third ventricle. In one patient, the tumor was centered more anteriorly in the third ventricle, without significant pineal cistern involvement. Five PBLs had tail-like extensions into the cerebral aqueduct, and PBLs rarely demonstrated parenchymal invasion. There were three ATRTs, of which two were centered in the cerebral hemispheres and one in the pineal cistern. Of the remaining seven embryonal tumors, five were centered in the cerebral hemispheres and two located within the lateral ventricles (Fig 1). The hemispheric embryonal tumors included three CNS_NB, one HGNET_MN1 and one ET, NOS; while the two lateral ventricular embryonal tumors included one each of ETMR and MB_WNT subtypes.

In the HGG subgroup, 16 out of 17 tumors primarily involved the cerebral hemispheres, and one was centered in the lateral ventricle. Both of the molecularly diagnosed EP were centered in the cerebral hemispheres.

MRI features were compared between the two broad groups -- PBL/ET and non-ET (Table 3). The median tumor size for the non-ET group was 6.2 cm (range 2.7–9.3) while that for PBL/ET group was 3.6 cm (range 1.1–9.1), and the difference was statistically significant ($p<0.001$). Thirty-two percent of tumors in the non-ET group (6/19) had ill-defined margins, compared to none in the PBL/ET group ($p<0.001$). Of note, all six tumors with ill-defined margins were HGG. Perilesional edema was seen in 74% of the non-ET group (14/19) compared to 14% in the PBL/ET group (5/37), also statistically significant ($p<0.001$). Enhancement was seen in nearly all tumors in both non-ET (19/19) and PBL/ET (36/37) groups, although 47% of tumors in the non-ET group had >75% enhancement, compared to 73% of tumors in the PBL/ET group ($p=0.08$), suggesting a tendency for more homogenous enhancement in PBL/ET. Majority of tumors in both groups demonstrated restricted diffusion, cysts/necrosis and calcification/hemorrhage, with no significant differences for any of these parameters (Table 3).

None of the non-ET patients had intracranial or intraspinal metastasis identified by MRI, while 32% of PBL/ET patients (12/37) had metastasis by MRI (one intracranial, five intraspinal and six both) (Table 3). One patient in each of the non-ET and PBL/ET group had positive CSF cytology, but no detectable metastasis by MRI.

After excluding PBL, statistical associations were examined between the remaining ET (n=10) and non-ET (n=19). The median age at diagnosis for this ET subgroup was slightly lower (8.4 years) compared to non-ET group (11 years), although the difference was not statistically significant ($p=0.10$). None of the studied MRI parameters showed any statistically significant differences, although we observed some trends (Table 4). Ill-defined margins were observed in 31.6% of non-ET, compared to none in the ET group. Calcification/hemorrhage was more commonly seen in non-ET (73.7%) compared to ET (40%).

A univariable analysis of imaging parameters with EFS was performed (Fig 2). Larger tumor size and ill-defined margins were statistically significant predicators of worse outcomes (p=0.023 and 0.006 respectively).

Discussion:

To our knowledge, this is the largest series describing the MRI findings of histologically diagnosed supratentorial 'PNET' and PBL, and the first one to correlate MRI features with molecular diagnoses and patient outcomes.

The rapid advances in understanding of the genomic characteristics of tumor cells have led to reassessment of tumor classification and traditional risk factors.[19,20] In particular, both supra and infra-tentorial embryonal tumors are moving from traditional histology only-based approach to molecular diagnoses for risk stratification and treatment planning. [7,16,22,23] In keeping with the new classification systems, there is a need to change the reference point of oncologic imaging from histopathology to molecularly integrated diagnoses.

The above numbers highlight that using histopathology only for diagnosis, 39% of all tumors (17 HGG, 2 EP and 3 ATRT out of total 56) and 71% of non-pineal tumors (16 HGG, 2 EP, 2 ATRT out of total 28) on this study represented discrepant molecular diagnoses not intended for inclusion on this 'PNET' trial. Our previously published results have shown markedly worse outcomes for these non-ET [7] despite a much smaller incidence of CSF dissemination by imaging and CSF cytology (5% for non-ET versus 35% for PBL/ET).

The majority of pineal region tumors in our study were confirmed to be pineoblastomas (Fig 3 and Fig 4). The pineal region ATRT in our study could not be subjectively distinguished from PBL (Fig 3). Also, there was one HGG in the pineal region which interestingly belonged to methylation class of diffuse midline glioma H3K27M mutant. Of the non-pineal tumors, which include both hemispheric and ventricular locations, only 43% belonged to the embryonal group, with the remainder being HGG and EPN (Table 2); with substantial overlap in the imaging appearances (Fig 5 and 6).

The median age (9 years) in this study was higher than previously reported for supratentorial PNET (6.5 years).[4] The median age at diagnosis for pineoblastomas (8.7 years) in our study is also higher than a recent large series (5.5 years).[24]

With all locations included, the non-ETs were larger, with more ill-defined margins and surrounding edema compared to the PBL/ETs. This may be partly related to location, with pineal region tumors probably presenting earlier because of hydrocephalus, although tumor biology and rate of growth could be contributing factors. After excluding pineoblastomas, none of the MRI parameters were statistically significant between the remaining ET and non-ET, however the ET had a tendency towards less heterogeneity, better defined margins, and occurred at a slightly younger age compared to non-ET.

Because of the rarity of these tumors, there are only a few published reports on their imaging features.[25–28] The PBL in our study demonstrated MRI features broadly similar to previous

descriptions, including diffusion restriction, cystic/necrotic change and variable enhancement. Parenchymal invasion however was rare in our study, which conflicts with one of the prior reports.[27] An 'aqueductal tail' was seen in 19% of PBL (Fig 3 and 4). Other than a single case report on PBL[29], this finding has not been mentioned in any of the previous descriptions of PBL or pineal region germ cell tumors. Although such a 'plastic' tumor extension is well-described for infratentorial ependymomas,[30] neither of the two molecularly diagnoses EPN in our study were seen in the pineal region. This observation can be explored on future studies to potentially distinguish PBL from other pineal region masses, which has always been considered difficult by imaging. [31,32]

CNS-PNET have typically been described on imaging as large, heterogeneous, diffusion restricting hemispheric or ventricular masses in young children.[28] No studies have compared the imaging findings to other malignant supratentorial tumors like high grade gliomas. A report from the German multicenter HIT trial compared the MRI findings of ependymoblastomas and ependymomas to CNS-PNET NOS. Although they found some differences by imaging, their overall conclusion was that precise distinction in individual cases may not be feasible.[33]

The study has several limitations that must be acknowledged. Methylation profiling was not available on all enrolled patients, and some additional patients were excluded because of inadequate imaging. The MRI techniques were not standardized, and quantitative assessments such as ADC measurements were not performed. The patients received different treatments based on the trial protocol, and that could potentially confound the correlation with outcomes, although there were no significant differences in the outcomes between treatment groups in our primary analysis.[7] Radiologically, these supratentorial tumors can be viewed as two groups based on location - pineal and extra-pineal, however they were included together for analysis because of shared histopathology and their designation as a single entity by neuro-oncologists for treatment purposes. Since, majority of the pineal region tumors eventually were proved to be pineoblastomas and majority of the non-pineal tumors were non-embryonal, including these together skews the statistical results. We also did a separate statistical analysis of ET versus non-ET after excluding pineoblastomas, which is more of a diagnostic dilemma from a radiological standpoint.

Conclusions:

We describe the imaging features of a large cohort of histologically diagnosed supratentorial 'PNET' including pineoblastomas in correlation with the molecular diagnoses and outcomes. Knowledge of current molecularly defined tumor entities, their relative frequencies and location will help the radiologist make more accurate predictions of the tumor types. For non-pineal tumors, a diagnosis of non-ET such as HGG or EPN should be high on the list of radiographic differential. Given the overlap of MRI findings, it may not be possible to offer a single diagnosis with certainty, and as such imaging does not substitute the need for obtaining molecular testing. However, a narrower differential diagnosis in conjunction with initial histopathology will be more helpful in guiding the surgery and radiation planning, and the gold standard molecular testing should guide the eventual course of treatment. The current study provides a systematic description of conventional MRI

findings in reference to the molecular diagnoses, and future studies in this direction using advanced imaging and radiomic techniques may be useful.

Acknowledgements:

This study was supported by the following:

NCTN Operations Center Grant U10 CA180886

NCTN Statistics and Data Center Grant U10 CA180899

St. Baldrick's Foundation

Grant support:

Supported in part by National Institutes of Health Grants No. U10-CA180886 (National Clinical Trials Network [NCTN] Operations Center Grant), U10-CA180899 (NCTN Statistics and Data Center), and grant from the St. Baldrick's Foundation.

Abbreviation key:

PNET	Primitive neuroectodermal tumor
ET	Embryonal tumor
PBL	Pineoblastoma
HGG	High grade glioma
EP	Ependymoma
ATRT	Atypical teratoid rhabdoid tumor

References:

1. Rorke LB. The cerebellar medulloblastoma and its relationship to primitive neuroectodermal tumors. J Neuropathol Exp Neurol 1983;42:1–15. [PubMed: 6296325]
2. Rorke LB, Trojanowski JQ, Lee VMY, et al. Primitive neuroectodermal tumors of the central nervous system. Brain Pathol 1997;7:765–84. [PubMed: 9161728]
3. Jakacki RI, Burger PC, Kocak M, et al. Outcome and prognostic factors for children with supratentorial primitive neuroectodermal tumors treated with carboplatin during radiotherapy: a report from the Children's Oncology Group. Pediatr Blood Cancer 2015;62(5):776–783. [PubMed: 25704363]
4. Pizer BL, Weston CL, Robinson KJ, et al. Analysis of patients with supratentorial primitive neuro-ectodermal tumors entered into the SIOP/UKCCSG PNET 3 study. Eur J Cancer 2006;42: 1120–1128. [PubMed: 16632346]
5. Sturm D, Orr BA Toprak UH, et al. New brain tumor entities emerge from molecular classification of CNS-PNETs. Cell 2016;164(5):1060–1072. [PubMed: 26919435]
6. Schwalbe EC, Hayden JT, Rogers HA, et al. Histologically defined central nervous system primitive neuro-ectodermal tumours (CNS-PNETs) display heterogeneous DNA methylation profiles and show relationships to other paediatric brain tumour types. Acta Neuropathol 2013; 126(6): 943–946. [PubMed: 24212602]
7. Hwang EI, Kool M, Burger PC, et al. Extensive Molecular and Clinical Heterogeneity in Patients With Histologically Diagnosed CNS-PNET Treated as a Single Entity: A Report From the Children's Oncology Group Randomized ACNS0332 Trial. J Clin Oncol 2018; 36(34): 3388–3395.

8. Louis DN, Perry A, Reifenberger G, et al. The 2016 World Health Organization Classification of Tumors of the Central Nervous System: a summary. Acta Neuropathol 2016; 131: 803–820. [PubMed: 27157931]
9. Pajtler KW, Witt H, Sill M, et al. Molecular classification of ependymal tumors across all CNS compartments, histopathological grades, and age groups. Cancer Cell 2015;27: 728–743. [PubMed: 25965575]
10. Ramaswamy V, Remke M, Bouffet E, et al. Risk stratification of childhood medulloblastoma in the molecular era : the current consensus. Acta Neuropathol. 2016;131(6):821–831. [PubMed: 27040285]
11. Kuo MD, Yamamoto S. Next generation radiologic-pathologic correlation in oncology: Rad-Path 2.0. AJR Am J Roentgenol 2011;197(4):990–997. [PubMed: 21940590]
12. Kuo MD, Jamshidi N. Behind the numbers: decoding molecular phenotypes with radiogenomics-guiding principles and technical considerations. Radiology 2014;270(2):320–325. [PubMed: 24471381]
13. Diehn M, Nardini C, Wang DS, et al. Identification of noninvasive imaging surrogates for brain tumor gene-expression modules. Proc Natl Acad Sci USA 2008;105(13):5213–5218. [PubMed: 18362333]
14. Jamshidi N, Diehn M, Bredel M, et al. Illuminating radiogenomic characteristics of glioblastoma multiforme through integration of MR imaging, messenger RNA expression, and DNA copy number variation. Radiology 2014;270(1):1–2.
15. Perreault S, Ramaswamy V, Achrol AS, et al. MRI surrogates for molecular subgroups of medulloblastoma. AJNR Am J Neuroradiol 2014;35:1263–69. [PubMed: 24831600]
16. Nowak J, Nemes K, Hohm A, et al. Magnetic resonance imaging surrogates of molecular subgroups in atypical teratoid/rhabdoid tumor (ATRT). Neuro Oncol 2018;20(12):1672–1679. [PubMed: 30010851]
17. Karlo CA, Di Paolo PL, Chaim J et al. Radiogenomics of clear cell renal cell carcinoma: associations between CT imaging features and mutations. Radiology 2014; 270(2):464–471 [PubMed: 24029645]
18. Capper D, Jones DTW, Sill M, et al. DNA methylation-based classification of central nervous system tumors. Nature 2018; 555:469–74. [PubMed: 29539639]
19. Aryee MJ, Jaffe AE, Corrada-Bravo H, et al.: Minfi: A flexible and comprehensive bioconductor package for the analysis of Infinium DNA methylation microarrays. Bioinformatics 2014; 30:1363–1369. [PubMed: 24478339]
20. Gajjar A, Pfister SM, Taylor MD, et al. Molecular insights into pediatric brain tumors have the potential to transform therapy. Clin Cancer Res 2014; 20:5630–40. [PubMed: 25398846]
21. Zaky W Revisiting Management of Pediatric Brain Tumors with New Molecular Insights. Cell 2016;164(5):844–846. [PubMed: 26919424]
22. Leary SE, Olson JM. The molecular classification of medulloblastoma: driving the next generation clinical trials. Current opinion in pediatrics. 2012;24:33–9. [PubMed: 22189395]
23. Sin-Chan P, Li BK, Ho B, et al. Molecular classification and management of rare pediatric embryonal brain tumors. Curr Oncol Rep 2018; 20, 69. [PubMed: 29995179]
24. Parikh KA, Venable GT, Orr BA, et al. Pineoblastoma-the experience at St. Jude Children's Research Hospital. Neurosurgery 2017; 81: 120–128. [PubMed: 28327927]
25. Chawla A, Emmanuel JV, Seow WT, et al. Paediatric PNET: pre-surgical MRI features. Clin Radiol 2007; 62:43–52. [PubMed: 17145263]
26. Klisch J, Husstedt H, Hennings S, et al. Supratentorial primitive neuroectodermal tumours: diffusion-weighted MRI. Neuroradiology 2000; 42:393–398. [PubMed: 10929296]
27. Nakamura M, Saeki N, Iwadate Y, et al. Neuroradiological characteristics of pineocytoma and pineoblastoma. Neuroradiology 2000;42:509–14. [PubMed: 10952183]
28. Dai AI, Backstrom JW, Burger PC, et al. Supratentorial primitive neuroectodermal tumors of infancy: Clinical and radiologic findings. Pediatr Neurol 2003;29(5):430–434. [PubMed: 14684239]
29. Fujita A, Asada M, Saitoh M, et al. Pineoblastoma showing unusual ventricular extension in a young adult—case report. Neurol Med Chir (Tokyo) 1999; 39: 612–616. [PubMed: 10487041]

30. Yuh EL, Barkovich AJ, Gupta N. Imaging of ependymomas: MRI and CT. Childs Nerv Syst 2009; 25: 1203–1213. [PubMed: 19360419]

31. Dumrongpisutikul N, Intrapiromkul J, Yousem DM. Distinguishing between germinomas and pineal cell tumors on MR imaging. AJNR Am J Neuroradiol 2012; 33(3):550–555. [PubMed: 22173760]

32. Kakigi T, Okada T, Kanagaki M, et al. Quantitative imaging values of CT, MR, and FDG-PET to differentiate pineal parenchymal tumors and germinomas: are they useful? Neuroradiology 2014; 56 (4):297–303. [PubMed: 24510202]

33. Nowak J, Seidel C, Pietsch T, et al. Systematic comparison of MRI findings in pediatric ependymoblastoma with ependymoma and CNS primitive neuroectodermal tumor not otherwise specified. Neuro Oncol 2015;17(8):1157–1165. [PubMed: 25916887]

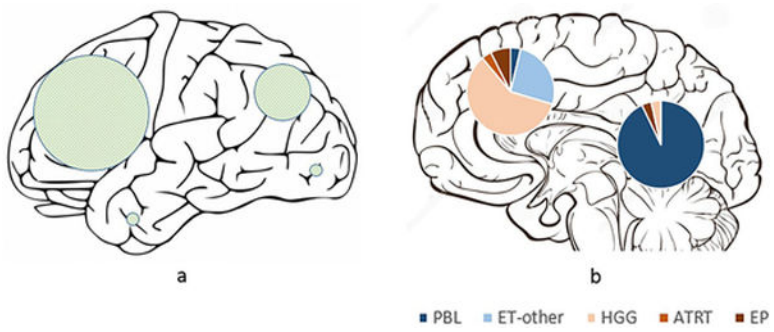

Fig 1.

Schematic representation of (a) the external surface of cerebral hemispheres showing the locations of hemispheric tumors, with the sizes of the shaded circles proportional to the number of tumors in each lobe; and (b) midline sagittal section of the brain showing pineal and non-pineal tumors, with pie diagrams representing the subgroups.

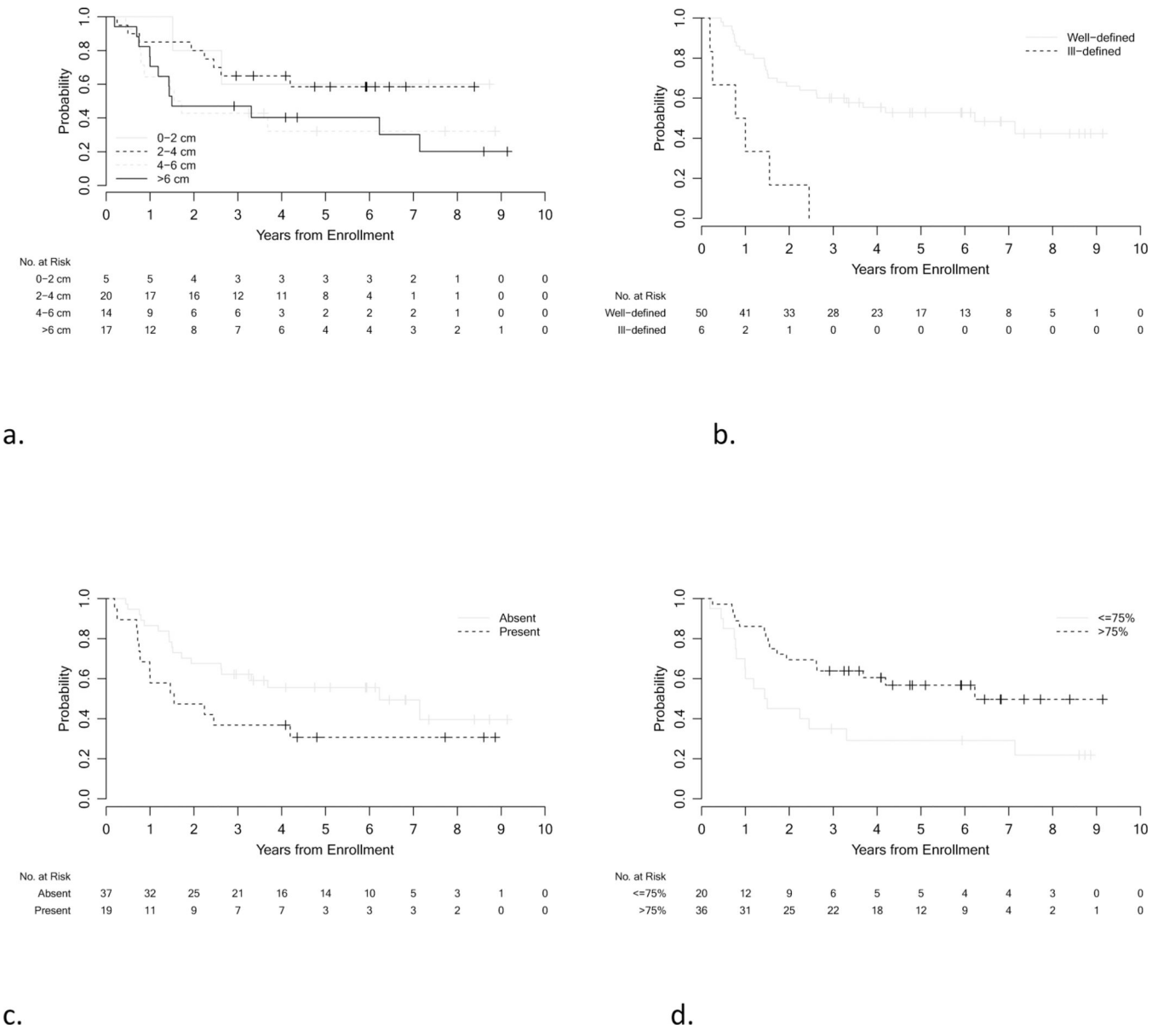

Fig 2.

Kaplan-Meier curves showing EFS distributions by tumor size (a), margins (b), presence of edema (c) and percent enhancement (d) for all patients (n=56).

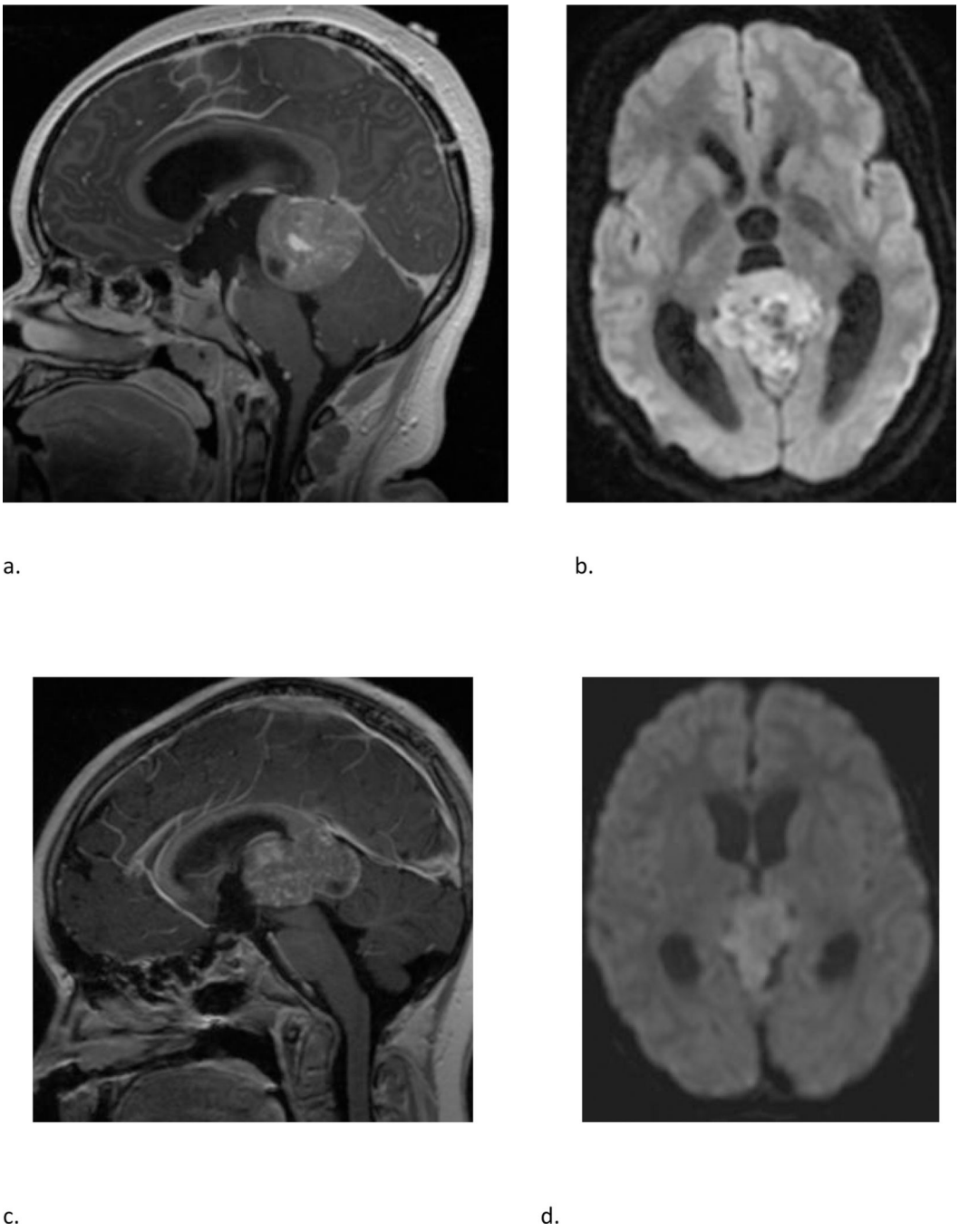

Fig 3 –.

(a & b) A 15 year-old-female with molecular diagnosis of pineoblastoma. Sagittal T1 weighted post contrast (a) and axial diffusion weighted (b) MRI images demonstrate a mass centered in the pineal region with diffuse heterogeneous enhancement, small cystic foci and diffusion restriction. (c & d) A 9-year-old female with molecular diagnosis of ATRT_MYC. Sagittal T1 weighted post contrast (c) and axial diffusion weighted (d) images demonstrate a similar mass centered in the pineal region with diffuse heterogeneous enhancement, small

cystic foci and diffusion restriction. Note the similarities in imaging appearance between the two examples.

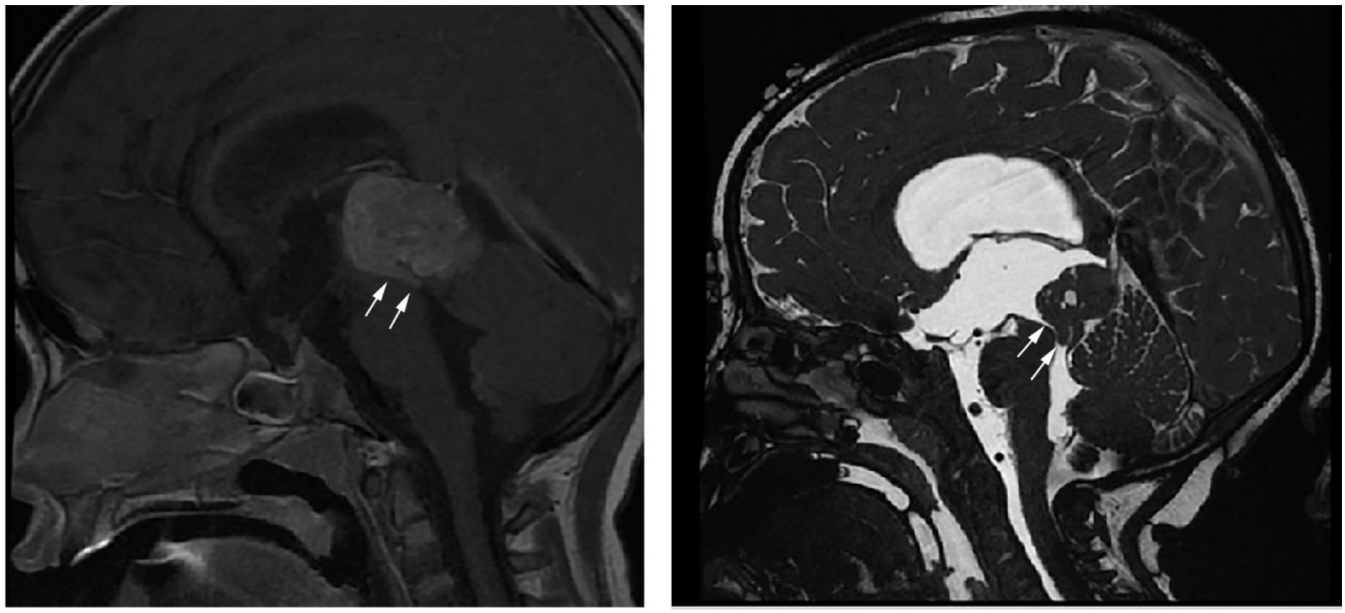

a. b.

Fig 4 –.

Sagittal T1 weighted post contrast (a) and sagittal high resolution balanced steady-state gradient echo (b) images from two different patients with molecularly proven pineoblastomas demonstrating tail like aqueductal extension (white arrows).

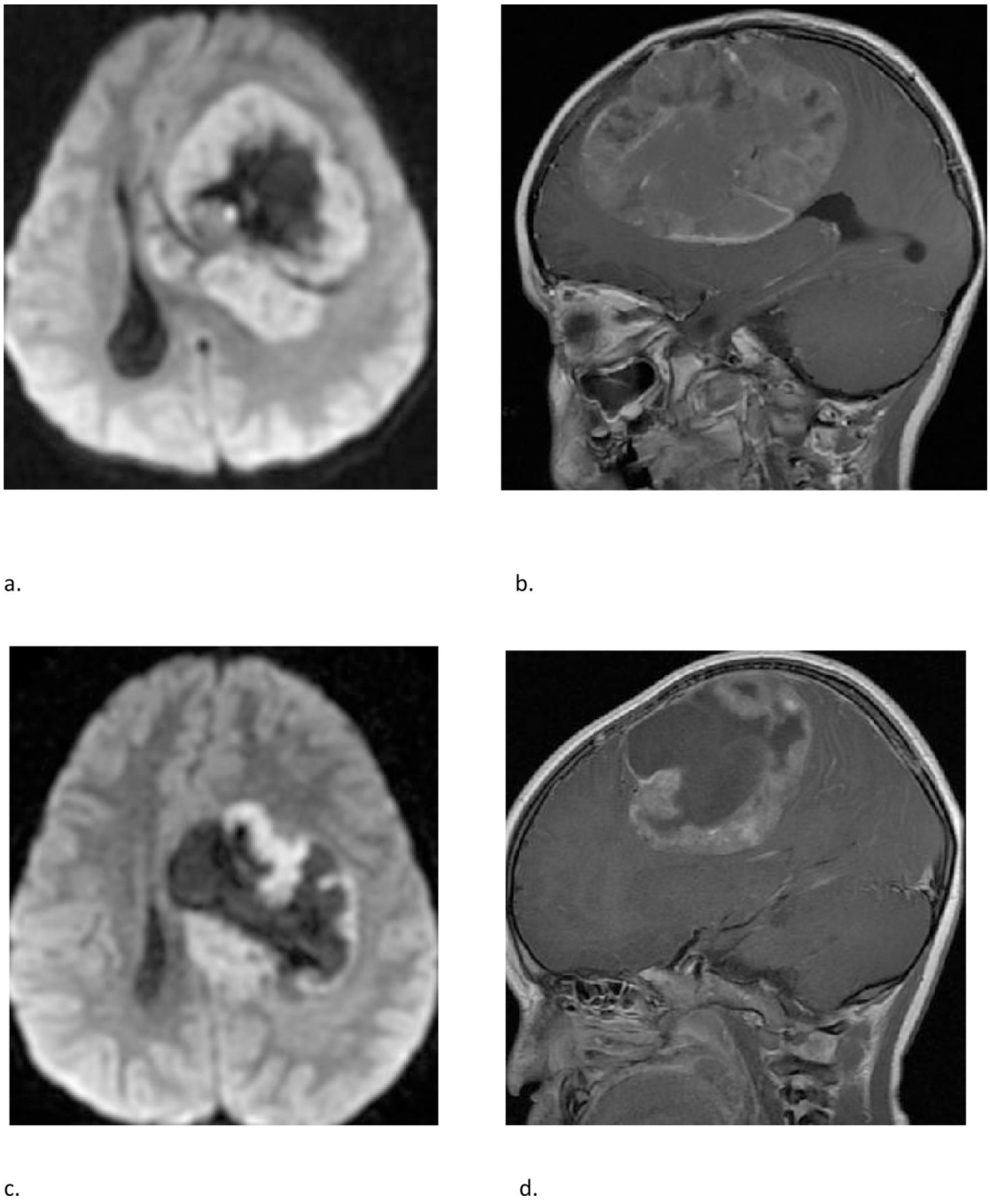

Fig 5 –.

(a & b) A 4-year-old female with molecular diagnosis of high grade glioma (GBM_MYCN). Axial DWI (a) and sagittal post contrast T1 weighted (b) images demonstrate a large mass centered in the left frontal lobe with prominent necrotic/cystic areas centrally; diffusion restriction and moderate heterogenous enhancement of the solid component. (c & d) A 4-year-old male with molecular diagnosis of ependymoma (EPN_RELA). Axial DWI (c) and sagittal post contrast T1 weighted (d) images demonstrate a large mass centered deep in the left hemisphere with prominent necrotic/cystic areas centrally; diffusion restriction and

moderate heterogenous enhancement of the solid component. Note the similarities in age and imaging appearance between these two cases with different molecular diagnoses.

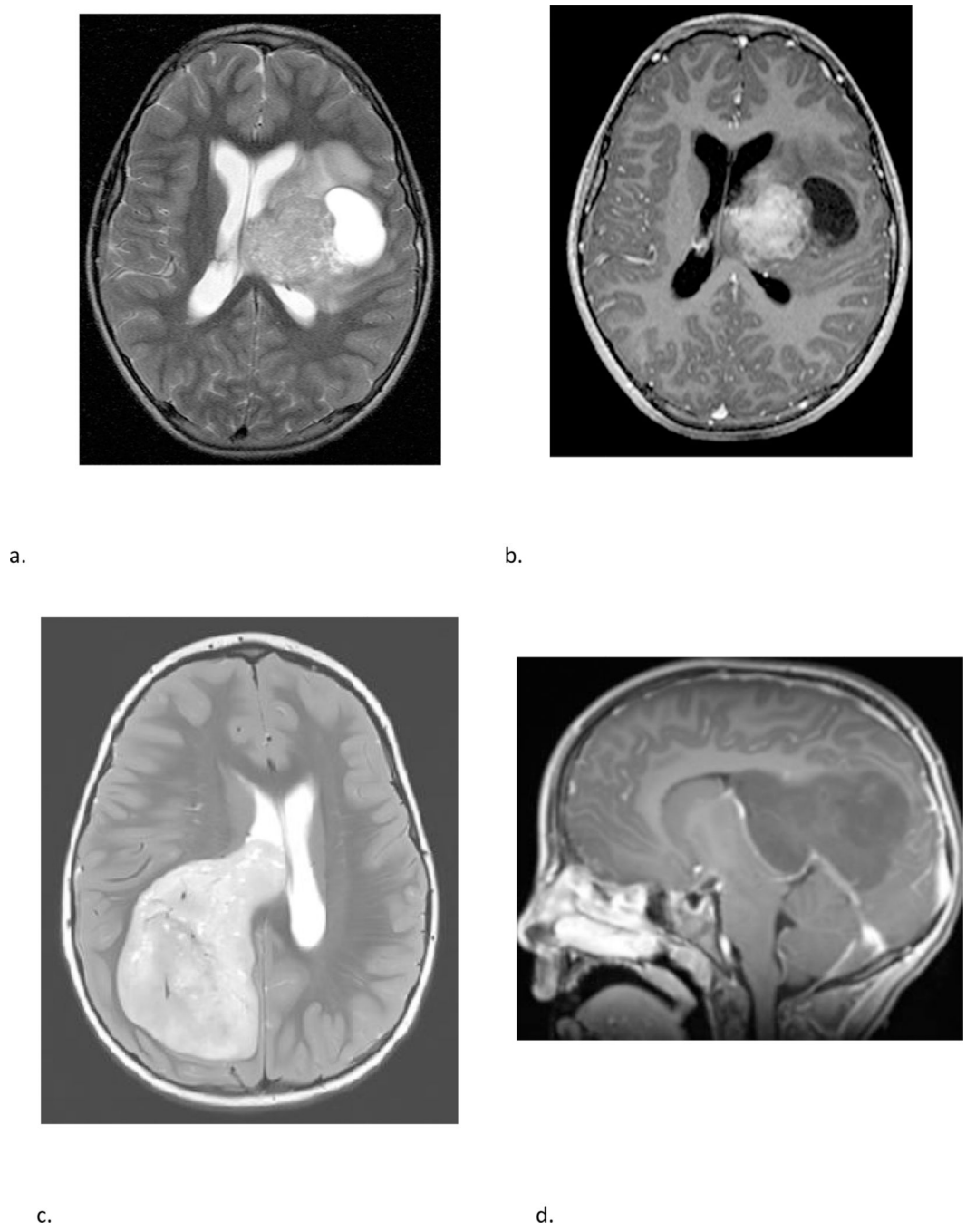

Fig 6 –.

Two different patients with molecular diagnosis of ET. (a & b) A 10-year-old female with axial T2 weighted (a) and axial post contrast T1 weighted (b) images demonstrating a large mass centered in the left deep nuclei with a prominent cystic component, and moderate enhancement of the solid component. The tumor subclass was CNS_NB_FOXR2. Please note the similarities with high grade glioma and ependymoma illustrated in fig 5. (c & d) A 5-year-old female with axial T2 weighted (c) and sagittal post contrast T1 weighted (d) images demonstrating a large solid mass centered in the right lateral ventricle with minimal

to no enhancement. The tumor subclass was ETMR. Of note, both these tumors demonstrated diffusion restriction (not shown).

Table 1.

Molecular diagnoses for tumors with both imaging and methylation profiles available (n=56).

PBL/ET	n	Non ET	n
PBL	27	*GBM_G34	8
~CNS_NB_FOXR2	3	*GBM_MYCN	5
~ETMR	1	*DMG_K27	2
~HGNET_MN1	1	*GBM-MID	2
~MB_WNT	1	EPN-RELA	2
~CNS ET, NOS	1		
^ATRT_SHH	2		
^ATRT_MYC	1		
Total	**37**		**19**

for further analysis, the following have been combined into single groups –

~as ET-other;

^as ATRT;

*as HGG

(PBL: Pineoblastoma; CNS_NB_FOXR2: CNS neuroblastoma with FOXR2 activation; ETMR: embryonal tumor with multilayered rosettes; HGNET_MN1: CNS high-grade neuroepithelial tumor with MN1 alteration; MB_WNT: medulloblastoma with wnt (wingless) activation; CNS ET, NOS: CNS embryonal tumor, not otherwise specified; ATRT_SHH: Atypical teratoid rhabdoid tumor with shh (sonic hedgehog) activation; ATRT_MYC: Atypical teratoid rhabdoid tumor, subclass MYC; GBM_G34: Glioblastoma, IDH wildtype, H3.3 G34 mutant; GBM_MYCN: Glioblastoma, IDH wildtype, subclass MYCN; DMG_K27: diffuse midline glioma H3K27M mutant; GBM-MID: Glioblastoma, IDH wildtype, subclass midline; EPN-RELA: Ependymoma with positive RELA fusion)

Table 2.

Molecular diagnoses for tumors by pineal and non-pineal locations.

	Pineal	Non-pineal
PBL	26	1
ET- other	0	7
ATRT	1	2
HGG	1	16
EP	0	2
Total	28	28

(PBL: Pineoblastoma; ET: Embryonal tumor; ATRT: Atypical teratoid rhabdoid tumor; HGG: High grade glioma; EP: Ependymoma)

Table 3.

MRI features by tumor group (all patients n=56).

	Group				*P*	All Patients	
	PBL/ET		Non-ET				
	n	%	n	%		n	%
Size (in centimeters)							
Median	3.6	-	6.2	-	<0.001	4.3	-
Minimum	1.1	-	2.7	-		1.1	-
Maximum	9.1	-	9.3	-		9.3	-
% Enhancement							
None	1	2.7	0	0	0.17[a] 0.080[b]	1	1.8
0 to 25	3	8.1	3	15.8		6	10.7
25 to 75	6	16.2	7	36.8		13	23.2
>75	27	73.0	9	47.4		36	64.3
Margins							
Well-defined	37	100.0	13	68.4	<0.001	50	89.3
Ill-defined	0	0	6	31.6		6	10.7
Presence of edema							
Absent	32	86.5	5	26.3	<0.001[c]	37	66.1
<2 cm from tumor margin	4	10.8	13	68.4		17	30.4
>2 cm from tumor margin	1	2.7	1	5.3		2	3.6
Presence of cyst/necrosis							
Absent	12	32.4	3	15.8	0.22	15	26.8
Present	25	67.6	16	84.2		41	73.2
Presence of calcification or hemorrhage						21	37.5
Absent	16	43.2	5	26.3	0.26	21	37.5
Present	21	56.8	14	73.7		35	62.5
Diffusion weighted imaging (DWI)							
Bright	28	75.7	15	78.9		43	76.8
Dark	1	2.7	0	0	--	1	1.8
Intermediate	5	13.5	3	15.8		8	14.3
Artifact or not available	3	8.1	1	5.3		4	7.1
Metastasis							
Intracranial	1	2.7	0	0		1	1.8
Spinal	5	13.5	0	0		5	8.9
Intracranial and spinal	6	16.2	0	0		6	10.7
None	25	67.6	19	100.0	--	44	78.6
All Patients	**37**	**100.0**	**19**	**100.0**		**56**	**100.0**

[a] comparison of none vs. 0–25% vs. 25–75% vs. >75%

[b] comparison of >75% vs. ≤75%

[c] comparison of absent vs. present

Table 4.

MRI features by tumor group after excluding pineoblastomas (n=29).

	Group				*p*	All Patients	
	ET		Non-ET				
	n	%	n	%		n	%
Size (in centimeters)							
Median	5.7	-	6.2	-	0.95	6.1	-
Minimum	3.6	-	2.7	-		2.7	-
Maximum	9.1	-	9.3	-		9.3	-
% Enhancement							
None	0	0	0	0		0	0
0 to 25	2	20	3	15.8		5	17.2
25 to 75	5	50	7	36.8		12	41.4
>75	3	30	9	47.4	0.68[a]	12	41.4
Margins							
Well-defined	10	100.0	13	68.4	0.068	23	79.3
Ill-defined	0	0	6	31.6		6	20.7
Presence of edema							
Absent	5	50	5	26.3	0.24[b]	10	34.5
<2 cm from tumor margin	4	40	13	68.4		17	58.6
>2 cm from tumor margin	1	10	1	5.3		2	6.9
Presence of cyst/necrosis							
Absent	0	0	3	15.8		3	10.3
Present	10	100	16	84.2	0.53	26	89.7
Presence of calcification or hemorrhage							
Absent	6	60	5	26.3	0.11	11	37.9
Present	4	40	14	73.7		18	62.1
Diffusion weighted imaging (DWI)							
Bright	9	90	15	78.9		24	82.8
Dark	0	0	0	0	--	0	0
Intermediate	0	0	3	15.8		3	10.3
Artifact or not available	1	10	1	5.3		2	6.9
Metastasis							
Intracranial	0	0	0	0		0	0
Spinal	0	0	0	0		0	0
Intracranial and spinal	0	0	0	0		0	0
None	10	100	19	100.0		29	100
All Patients	**10**	**100.0**	**19**	**100.0**		**29**	**100.0**

[a] comparison of none vs. 0–25% vs. 25–75% vs. >75%

[b] comparison of absent vs. present